

Dynamic NMR Study of the Kinetics of Complexation of Tl^+ Ion with Calix[4]crown-6

Hedayat Haddadi,[†] Naader Alizadeh,^{*,†} Mojtaba Shamsipur,[‡] and Zouhair Asfari[§]

Department of Chemistry, Faculty of Basic Science, Tarbiat Modares University, P.O. Box14115-175, Tehran, Iran, Departments of Chemistry, Razi University, Kermanshah, Iran, and Laboratoire de Chimie Analytique et Minerale, UMR 778, ULP/CNRS/IN2P3(LC4), ECPM, 25 Rue Becquerel, F-67087, Strasbourg Cedex, France

Received: February 24, 2010; Revised Manuscript Received: May 31, 2010

The complexation and exchange kinetics and mechanism for the dissociation and conformational change of thallium ion complex of calix[4]crown-6 were studied in $CD_3CN/CDCl_3$ (4:1 v/v) solution by dynamic 1H NMR. The results show the formation of a 1:1 complex with cone conformation. From variable temperature dynamic NMR analysis in the range 223–293 K, two coalescence temperatures at 228 and 243 K were ascertained. The activation parameters for the dissociation process, E_a (kJ/mol), ΔS^\ddagger (J/mol.K), and ΔH^\ddagger (kJ/mol) are 11.0, –133.2, and 10.1 for the bimolecular regime and 21.5, –112.8, and 20.6 for the unimolecular regime, respectively. In addition, the dynamic 1H NMR spectroscopy shows that the exchange of Tl^+ between the two crown sides of the complexed ligand proceeds through an intramolecular tunneling. An Arrhenius convex curve was observed for intramolecular exchange. This phenomenon is explained in terms of two conformer state formations differentiated by hydrogen bond association.

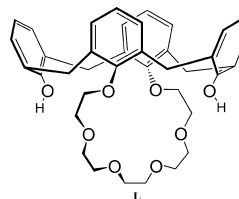
Introduction

Calixarenes are flexible macrocyclic compounds that are the focus of considerable interest as useful building blocks for the construction of relatively rigid lipophilic cation receptors and carriers with desired properties.^{1,2} Among the interesting properties of calixarenes and their derivatives, perhaps the prominent one is their binding ability with metal ions.³ The efficiency and selectivity in metal ion binding by calixarene ionophores depends not only on the ring size of the calix but also on the nature of the binding groups attached, nature of the cation, degree of deprotonation and, especially for calix-[4]arene derivatives, on the conformation of the macrocycle (cone, partial cone, 1,3-alternate, and 1,2-alternate).^{1,4–7}

It is well-known that natural ionophores such as valinomycin and monensin mediate alkali cation transport through biological membranes.^{8–10} Meanwhile, thallium(I) has long been proposed as a suitable probe for alkali metal cations, especially potassium ion, in biological systems due to its chemical similarity.¹¹ By a materials approach, there is an increasing interest on the chemistry as well as a number of potential applications of calixarene derivatives.¹² Formation of thallium complexes with different stoichiometry was reported earlier for calixarene derivatives.^{13–18}

To the best of our knowledge, there is no literature on the kinetics and mechanism of the formation and dissociation of thallium ion complexes with calix[4]arenes in solution. A deeper understanding of the factors affected and of the mechanisms responsible for the host–guest complexation in solution necessitates the studies on the thermodynamics and kinetics of the corresponding complexation and dissociation processes. Although many thermodynamic studies on the complexation processes of calixarenes have appeared in the past few years, kinetic and mechanistic studies are still scarce.¹⁹ In this paper,

SCHEME 1: The Structure of Calix[4] crown-6



we wish to report the results of proton NMR studies of the complexation of thallium(I) ion with calix[4]crown-6 (L, scheme 1), a fast exchange system, in a 4:1 (v/v) mixture of deuterated acetonitrile and chloroform. The activation parameters of the exchange kinetics were evaluated by using the simple Eyring and Arrhenius equations in the presence of excess ligand. However, the Arrhenius plot revealed a nonlinear convex shape for the $Tl^+ - L$ system at metal ion/ligand molar ratios ≥ 1 . The results of dynamic 1H NMR spectroscopy at low temperatures showed that this phenomenon is in fact an intramolecular event impeded by the steric effects of hydrogen bonding.

Experimental Section

1H NMR Spectroscopy and Conductometry. Variable temperature 1H NMR studies were carried out on a Bruker DRX-500 pulsed Fourier transform NMR spectrometer at 500 MHz, from 293 to 223 K, using 5-mm o.d. NMR tubes. The temperature of the probe was adjusted with a temperature-control unit, using liquid nitrogen at low temperatures and a heating element at high temperatures. To reach the equilibrium temperature, each sample tube was left in the probe for at least 10 min before measurements. At all temperatures used, the accuracy of the temperature measurement was ± 0.1 °C. The TMS signal in $CD_3CN/CDCl_3$ (4:1 v/v) was used as an internal reference for the 1H chemical shifts. The 1H NMR spectra were recorded with a 90° pulse width of 15.0 μs . The acquisition time and the delay between two pulses were 1.6 and 6.0 s, respectively. The concentration of ligand in all experiments was used 0.002 M.

* To whom correspondence should be addressed. Fax +98-21-82883455. E-mail: alizaden@modares.ac.ir.

[†] Tarbiat Modares University.

[‡] Razi University.

[§] ULP/CNRS/IN2P3(LC4).

Conductance measurement was carried out with a Metrohm 712 conductivity meter. A dip-type cell, made of platinum black, was used. During the conductance measurement, the cell were thermostatted using a circulating water bathes (Frigomix B. Braun UM-S) for adjusting the temperature with accuracy of ± 0.1 °C.

Chemicals and Solutions. Deuterated acetonitrile and chloroform were purchased from Armar Chemicals and were used throughout. Thallium perchlorate was synthesized according to the method of Coetzee et al. by reaction of thallium nitrate and perchloric acid.²⁰ The thallium salt was recrystallized three times from water and drying at 120 °C and store in vacuum desiccator over P_2O_5 . All other materials were purchased from Merck. The mixed solvents were dried over molecular sieve material before use (the water signal is not observed in 1H NMR spectra of solvent). Calix[4]crown-6 (**L**) was prepared and purified as described in our previous publication.²¹ The temperature-dependent 1H NMR spectra were subjected to complete line shape analyses using modified Bloch equations to obtain the temperature variation of the lifetimes.²²

Safety Note. Thallium compounds are highly toxic. Accordingly, appropriate personal protective equipment should be worn when handling thallium solutions to prevent accidental exposure. Thallium compounds are readily absorbed through various routes of exposure. The water-soluble salts are rapidly and completely absorbed from the respiratory tract, gastrointestinal (GI) tract, or skin (no information was found regarding the absorption of thallium salts via inhalation).^{23,24} Although we have not encountered any problems, it is noted that perchlorate salts of metal complexes with organic ligands are potentially explosive and should be handled only in small quantities with appropriate precautions.

Results and Discussion

Stability Constant Determination. In order to evaluate the formation constant of the $Tl^+ - L$ complex in a binary mixture of deuterated acetonitrile:chloroform (4:1 v/v), the proton NMR spectra of the ligand in the presence of different concentrations of Tl^+ ion were recorded at 296 K. The resulting chemical shift of the hydroxyl groups of **L** vs $[Tl^+]/[L]$ mole ratio (R) plot is shown in Figure 1A. As seen, only one average response signal was observed, indicating that the exchange rate of the cation between the bulk solution and the complexed site is fast on the NMR time scale at room temperature. Figure 1A clearly shows that an increase in the Tl^+ ion concentration gradually shifts the proton resonance of **L** hydroxyl groups upfield until a R value of about 1 is reached; further addition of the cation does not change the resonance frequencies considerably. This behavior is indicative of the formation of a stable 1:1 complex. The formation constant of the resulting complex was evaluated by the computer fitting of the mole ratio data to a previously derived equation, which relates the observed chemical shift to the formation constant (Appendix A).²⁵ The resulting $\log K_f$ value was found to be ≥ 5.0 .

The stoichiometry and formation of the resulting $Tl^+ - L$ complex was also determined by conductometric titration of 10 mL of 5.0×10^{-5} mol/L of Tl^+ solution with **L** in acetonitrile:chloroform (4:1 v/v). The best-fit to the conductometric data confirmed the stoichiometry and formation of $Tl^+ - L$ complex determined by the 1H NMR method (the details of the derivations are given in Appendix B). The resulting molar conductance versus the $[L]/[Tl^+]$ mole ratio plot is shown in Figure 1B.

Spectral Changes During Complexation. Figure 2 shows the 1H NMR spectra of ligand **L**, in the presence (A) and

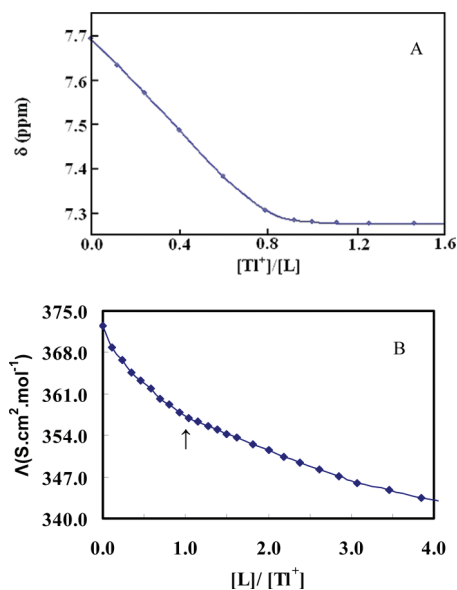


Figure 1. Proton chemical shift of the hydroxyl groups of **L** as a function of $[Tl^+]/[L]$ mole ratio in deuterated acetonitrile/chloroform (4:1) at 296 K (A). Molar conductance vs $[L]/[Tl^+]$ mole ratio in acetonitrile/chloroform at 296 K (B).

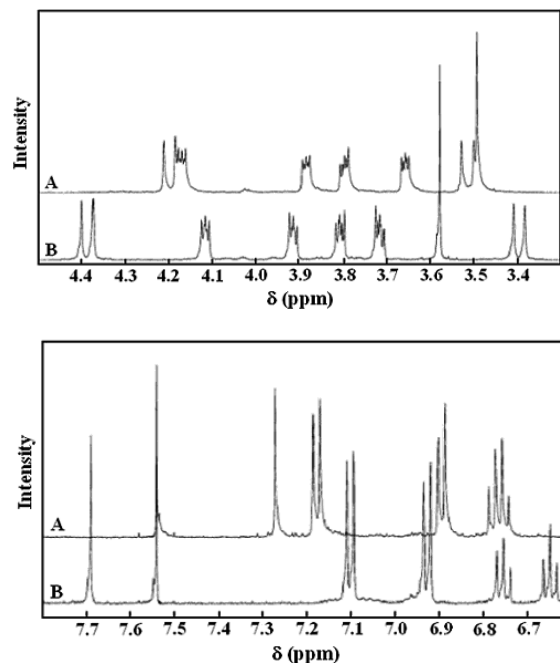


Figure 2. Proton NMR spectra of **L** in the presence (A) and absence (B) of Tl^+ ion.

absence (B) of 1:1 Tl^+ ion in deuterated acetonitrile/chloroform (4:1 v/v) at 296 K. The NMR spectral characteristics of the uncomplexed **L**, with **L** being in the cone conformation (Figure 2B), are summarized as follows: δ 7.69 (s, 2, ArOH), 7.10 (d, 4, ArH), 6.92 (d, 4, ArH), 6.75 (t, 2, ArH), 6.65 (t, 2, ArH), 4.38 (br d, 4, ArCH₂Ar), 3.7–4.1 (m, 16, OCH₂), 3.57 (s, 4, OCH₂), 3.39 (br d, 4, ArCH₂Ar).

The chemical shifts of the hydroxyl groups could be affected by a number of factors, such as polarity of a solvent, presence of traces of water, acids or bases, participating of groups in hydrogen bonding, temperature, and presence of a cation. However, it is known that calix[4]arenes with two hydroxyl groups at lower rim of calix[4]arene platform (like in ligand **L**) are stabilized in cone conformation due to hydrogen bonding between the hydroxyl groups.¹

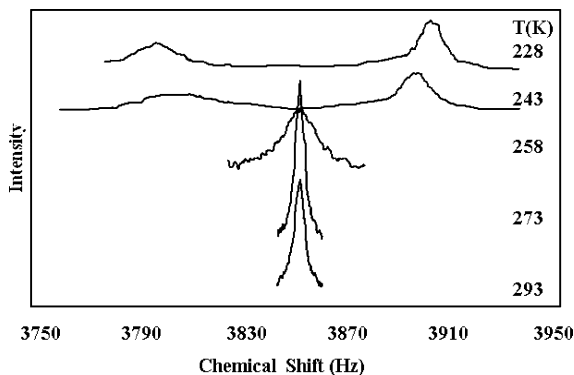


Figure 3. Typical proton NMR spectra of the Ti^+-L complex at various temperatures for a mixture of $[\text{L}] = 0.002 \text{ M}$ and $[\text{Ti}^+] = 0.001 \text{ M}$ in deuterated acetonitrile/chloroform (4:1).

As observed in Figure 2, the symmetry of the NMR signals corresponds to the possibly restricted geometry of Ti^+-L complex in solution. The largest shift of -0.41 ppm , from 7.69 to 7.28 ppm, was observed for the OH-bearing phenyl signal of **L** upon complexation with Ti^+ ion, reflecting the strong interaction of Ti^+ ion with the hydroxyl groups of **L**. The singlet at 7.28 ppm at a molar ratio of 1 is assigned to the phenolic protons of Ti^+-L complex. Four multiplet signals with equal integrals at around 3.7–4.1 ppm can be attributed to the $-\text{CH}_2-$ groups of the crown loop, and also a singlet at 3.57 ppm can be assigned to the two equivalent neighboring $-\text{CH}_2-$ groups of the crown loop (spectrum B). The benzylic protons signals showed the AB systems (at 3.39 and 4.38 ppm) indicating the cone conformation of this diphenol. However, the benzylic coupling for the diphenol (NMR in $\text{CD}_3\text{CN}/\text{CDCl}_3$ (4:1 v/v), $J = 13 \text{ Hz}$) and chemical shift difference between two benzylic protons ($\Delta\delta = 1.01 \text{ ppm}$) clearly indicate its presence in the cone conformation (spectrum B).^{26,27} The remaining portion of the spectrum showed four sharp aromatic signals, two doublets (7.10 and 6.92 ppm), and two triplets (6.75 and 6.65 ppm).

Dynamic ^1H NMR Studies. The kinetics of the complexation of Ti^+ ion at lower temperature range of 223–293 K was investigated in the deuterated acetonitrile/chloroform (4:1 v/v) binary solvent system. The ^1H NMR spectrum of **L** in $R = 0$ exhibits very well separated signals for the crown and benzylic protons at temperature ranges of 223–293 K, indicating that the cone conformation is stabilized by the presence of circular arrays of intramolecular hydrogen bonds. Such a stabilization of a given conformation by hydrogen-bonding because of rigidifying of the host molecule and consequent reduction of exchange rates, has already been reported in the literature.^{28–32} Figure 3 depicts the representative proton NMR spectra of Ti^+-L system of a metal/ligand molar ratio of 0.5 at different temperatures. The observation of a pair of broad peaks corresponding to a metal/ligand molar ratio of 0.5 at low temperatures is also in support of the above discussion (Figure 3). It should be noted that the spectra at a metal/ligand molar ratio of 1.0 became a simple pattern again, where the spectrum is assigned to the cone conformation of the resulting complex. At higher metal/ligand molar ratios than 1.0 (i.e., up to 3.0), no further spectral change was observed. As it can be seen from Figure 3 (metal/ligand molar ratio of 0.5), the decrease in temperature from 293 to 223 K induces some changes in the ArOH signal and causes the single average signal, resulting from fast OH resonance, to separate into two signals, for free and complexed ligands, under a slow exchange protocol. The same changes were also observed for aromatic signals. Additional changes in the aliphatic region of the proton NMR spectra were difficult to interpret, due to

the broadness and overlapping of the signals. Consequently, for the exchange of thallium ion, we may assume the following two-site exchange system:

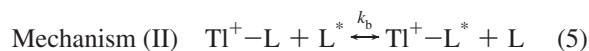
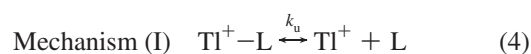


Equation 1 is meant for a general situation of the dissociation process and does not imply any specific mechanism for the exchange system. The activation parameters E_a , ΔH^\ddagger , and ΔS^\ddagger for the dissociation of the complex were evaluated from the Arrhenius and Eyring eqs 2 and 3, at Ti^+/L molar ratios < 1.0 .

$$k = A \exp[-(E_a/RT)] \quad (2)$$

$$k/T = (k_b/h) \exp[(-\Delta H^\ddagger/RT) + (\Delta S^\ddagger/R)] \quad (3)$$

Thus, it may be taken into account the possibility of the two following dissociation mechanisms for the Ti^+-L complex:³³



The first one is referred to as a unimolecular dissociation mechanism, and the second is a bimolecular ligand exchange, also known as an associative exchange mechanism. The general expression for the mean lifetime (τ) of the ligand in terms of mechanisms (I) and (II) is:

$$1/\tau = 2k_b[\text{L}]_t + k_u[\text{L}]_t/[\text{L}]_f \quad (6)$$

where $[\text{L}]_t$ and $[\text{L}]_f$ are the total concentration of the ligand and the concentration of uncomplexed ligand, respectively. Therefore, we can determine the relative contribution of the two dissociation mechanisms by the study of concentration dependence of the life times of the Ti^+-L complex. Mechanism (I) predicts the linear dependence of $1/\tau$ upon the relative population of the free ligand, whereas mechanism (II) predicts the linear dependence of $1/\tau$ upon the total concentration of the ligand. Thus, when the exchange process proceeds via a dissociative pathway, the $1/\tau[\text{L}]_t$ versus $1/[\text{L}]_f$ plot results in a straight line that passes through the origin, whereas in the case of the predominance of a bimolecular mechanism the plot results in a line parallel to the $1/[\text{L}]_f$ axis. The corresponding k_b and k_u values for the two exchange mechanisms can then be evaluated from the intercept and slope of the plots of $1/\tau[\text{L}]_t$ versus $1/[\text{L}]_f$, respectively.

To evaluate the mean lifetime (τ) at different mole ratios and temperatures, a nonlinear least-squares program was used to fit 100–200 points of the spectral data of the phenolic protons of **L** to the exchange equations (modified Bloch equations).^{22,33} The line widths of the free and complexed ligands were measured by fitting a Lorentzian function to their spectra of the phenolic protons of **L**. The modified Bloch equations can be obtained for an uncoupled two-site exchange of the free (**L**) and complexed ligand (Ti^+-L), the details are given in Appendix C.

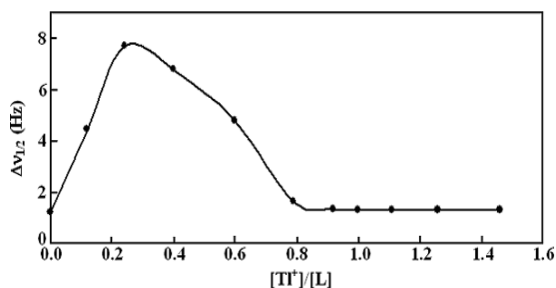


Figure 4. Concentration dependence of the peak width of $-\text{OH}$ protons of calix[4]crown-6 at 296 K.

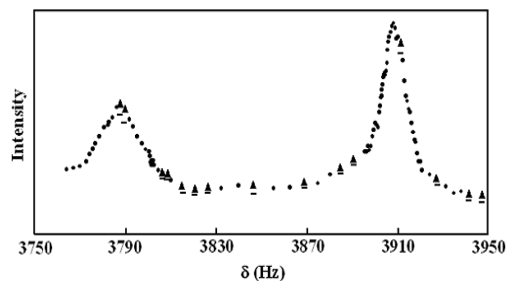


Figure 5. Typical representation of experimental and calculated proton NMR spectra of $-\text{OH}$ protons L at $R = 0.5$ and 223 K: (•) calculated and observed signal are equal, (▲) observed signal, (⊖) calculated signal.

Study of the Interaction of Tl^+ Ion with L at Metal/Ligand Mole Ratios $R < 1$. The signals at 7.70 and 7.28 ppm are ascribed to the free and complexed species of L , respectively (Figure 2). Figure 4 shows the concentration dependence of the peak width of OH protons of calix[4]crown-6 at 296 K. As can be seen, the chemical shift and the line width of the complexed signal is affected by an increase in the concentration of Tl^+ . This exchange pattern permits an easy test of the exchange mechanism.³⁴ These results allow discrimination between the two possible mechanisms for the decomplexation of the Tl^+-L complex. As is evident from Figure 4, the plot of line width as a function of the $R = [\text{Tl}^+]/[\text{L}]$ ratio passes through a maximum at $R = 0.3$, and the curve is not symmetrical with respect to this maximum, under conditions of a quantitative complex formation. It should be noted that, in the case of an associative interchange mechanism, the variations in line width should be symmetrical with respect to a maximum at $R = 0.5$.

Figure 5 shows the experimental and calculated proton NMR spectra of L at $R = 0.5$ and 223 K. The two observed signals are due to hydroxyl protons of the free (lower field) and complexed species L (higher field), under slow exchange conditions. The life times (τ) of the thallium complex were obtained using the complete line shape analysis for two-site exchange of L between the free and complexed sites.^{33,35} Figure 6 shows the concentration dependence of the relaxation times τ of the thallium complex at low temperatures of 228 and 223 K. As is evident from Figure 6, over the molar ratio range of $R = 0.25-0.50$ ($1/[\text{L}]_f = 666-1000$), the life times of the Tl^+-L complex are almost constant while in the range of $R = 0.5-0.75$ ($1/[\text{L}]_f = 1000-2000$), the life times (τ) increased by increasing concentration of the thallium complex. The results indicate that, for R values ≤ 0.5 , a bimolecular mechanism is dominated in the dissociation of the Tl^+-L complex, whereas for a range of $0.5 \leq R \leq 0.75$ an unimolecular pathway is the dominant mechanism at low temperatures. The corresponding k_b and k_u values for the two exchange mechanisms can then be evaluated according to eq 6. The corresponding Arrhenius plots are shown in Figure 7, and the resulting relaxation times, rate constants,

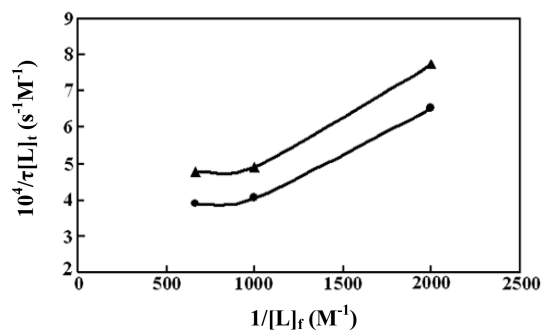


Figure 6. Concentration dependence ($[\text{L}]_f$: 0.0015, 0.001, and 0.0005 M) of the relaxation times (τ) of the thallium complex at low temperatures of 228 K (▲) and 223 K (•).

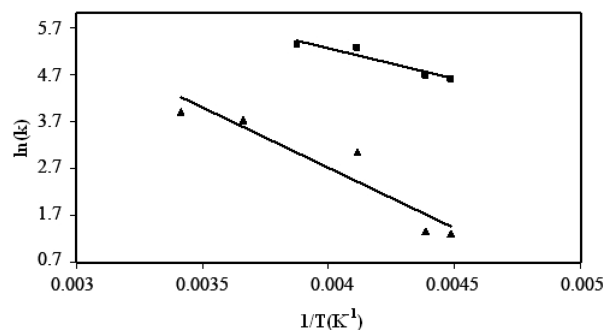


Figure 7. Arrhenius plots of Tl^+-L complex for $R < 1$: (■) bimolecular ligand exchange; (▲) unimolecular ligand exchange.

and activation parameters (E_a , ΔH^\ddagger , and ΔS^\ddagger) for the unimolecular and bimolecular exchange mechanisms are summarized in Table 1.

Study of the Interaction of Thallium and L at Mole Ratios $R \geq 1$. Figure 8 shows the proton NMR spectra, in the region 3.3–3.5 ppm, of Tl^+-L complex at different temperatures in the presence of excess Tl^+ ion. As seen, by a decrease in sample temperature, the single signal of OCH_2 of crown loop broadens and splits into two lines of equal integrals. It can be inferred that there are two exchangeable sites for methylene protons over the entire temperature range studied. The exchange is apparently quite swift even at 223 K. This observation can be interpreted in two different ways: (i) Tl^+ is bound to one of the two sides of crown loop, and the two binding sites are actually inequivalent (see Scheme 2), but they appear equivalent due to rapid ligand exchange. (ii) Tl^+ occupies the central position in the crown loop cavity, so that the complex is symmetric and all OCH_2 groups and benzene rings become equivalent to those of free ligand. If explanation (ii) is correct, a symmetrical signal pattern should appear at lower temperatures. As can be seen, the coalescence of signals for OCH_2 groups, especially the singlet of two neighboring OCH_2 , were observed at 228 K. Thus, the explanation (ii) is not correct because of incompatibility of this hypothesis with the observed unsymmetrical signals.

In addition, the explanation (i) can occur in two different ways: (a) hopping of Tl^+ ion between the two binding sites via an intermolecular metal exchange process or (b) intramolecular alternations of Tl^+ ion between the two binding sites through a δ hole of crown. To discriminate between these two possibilities, we examined the influence of the metal concentration on the relaxation times of the exchange process at different temperatures (Figure 9 and Table 2). If route (a) is dominant, $1/\tau$ should be increased linearly with free Tl^+ concentration (eq 7), with a slope of $2k_{bM}$, and if route (b) is dominant a straight line with an intercept of $2k_u$, or concentration-independent of life times should

TABLE 1: Life Times, Calculated Rate Constants, and Activation Parameters for Unimolecular and Bimolecular Exchange Mechanism in $R < 1$ from the Half Width of the $-OH$ Protons of L ($[L] = 0.002$ M)

T (K)	τ (ms)			exchange rate constants		activation parameters				
	$R = 0.25$	$R = 0.50$	$R = 0.75$	k_b ($M^{-1}s^{-1}$) ^a	k_u (s^{-1}) ^b	A (Hz)	E_a (kJ/mol)	ΔH^\ddagger (kJ/mol)	ΔS^\ddagger (J/molK)	ΔG_{258}^\ddagger (kJ/mol)
223	12.9	12.4	7.71	3.95×10^4	20.7					
228	10.5	10.2	6.47	4.83×10^4	23.6	3.82×10^4 ^a	11.0 ^a	10.1 ^a	-133.2 ^a	33.3 ^a
243	2.1	3.9	0.3	1.82×10^5	1081.3					
258	0.9	6.0	24.2	2.14×10^5						
273	0.5	0.08	72.0		5131.7	4.61×10^5 ^b	21.5 ^b	20.6 ^b	-112.8 ^b	49.7 ^b
293	0.1	0.06	63.5		8363.6					

^a Bimolecular regime. ^b Unimolecular regime.

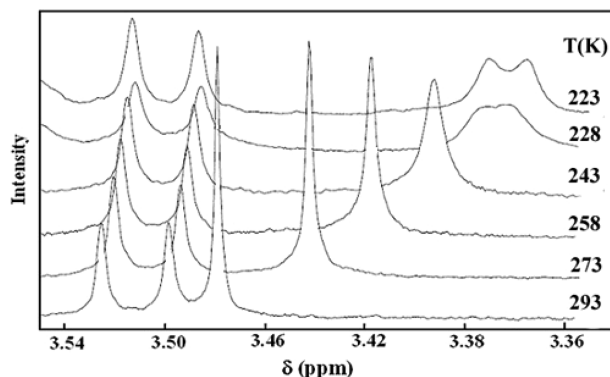
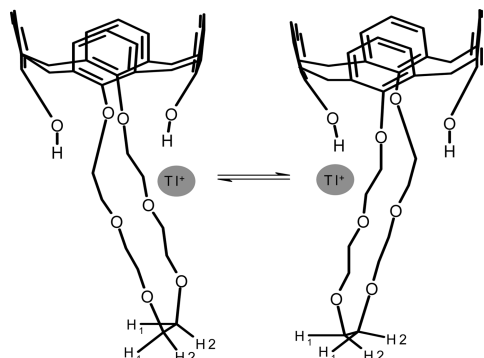


Figure 8. Proton NMR spectra of $Tl^+ - L$ complex at $R = 1.46$ in the region 3.3–3.5 ppm at different temperatures.

SCHEME 2: Flip-Flop-Type Motion of Thallium Ion through the Crown Hole of Calyx[4]crown-6



result (eqs 8).³³ As is seen from Figure 9, the results show the concentration-independence of life times, emphasizing on the occurrence of an intramolecular exchange of Tl^+ through the δ hole of crown or a flip-flop-type motion.³⁶ These results implied that the metal cation bound to the calix[4]crown-6 tends to dissociate intermolecularly into the solvent rather than to move

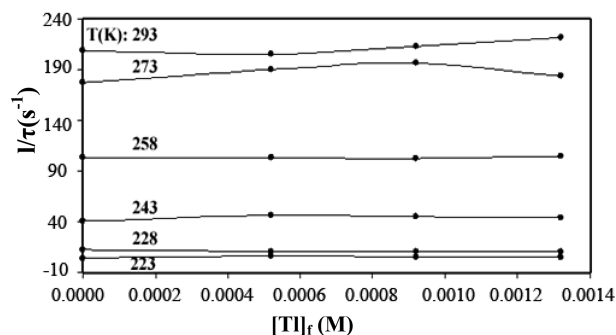


Figure 9. Influence of the metal concentration on the relaxation times for $R \geq 1$ at different temperatures.

intramolecularly to another side of the crown loop. So the elimination of two exchange sites caused by intramolecular event does not affect significantly in calculation of relaxation times of intermolecular kinetics for $R < 1$.

$$1/\tau = 2k_{bM}[Tl]_f \quad (7)$$

$$1/\tau = 2k_t \quad (8)$$

The Occurrence of Convex Arrhenius Curve and Its Interpretation.

To obtain information about the activation parameters of the exchange reaction, the Arrhenius plot of $\ln(k)$ vs $1/T$ was constructed and is shown in Figure 10. The observed slope of the Arrhenius plot at higher temperatures is smaller than that at lower temperatures. A literature survey reveals the presence of a few reports on the convex temperature behavior of rate constants in chemical and biological systems.^{37–42} Kohen et al. have interpreted this phenomenon by means of theoretical and experimental observations.³⁷ A convex Arrhenius curve means that by increasing temperature, the activation energy decreases. This phenomenon can be explained by Tolman's interpretation of the activation energy, which may be written as:^{43–45}

$$E_a = \bar{E} - \bar{E} \quad (9)$$

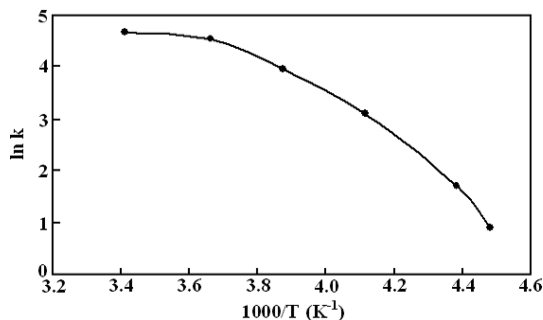
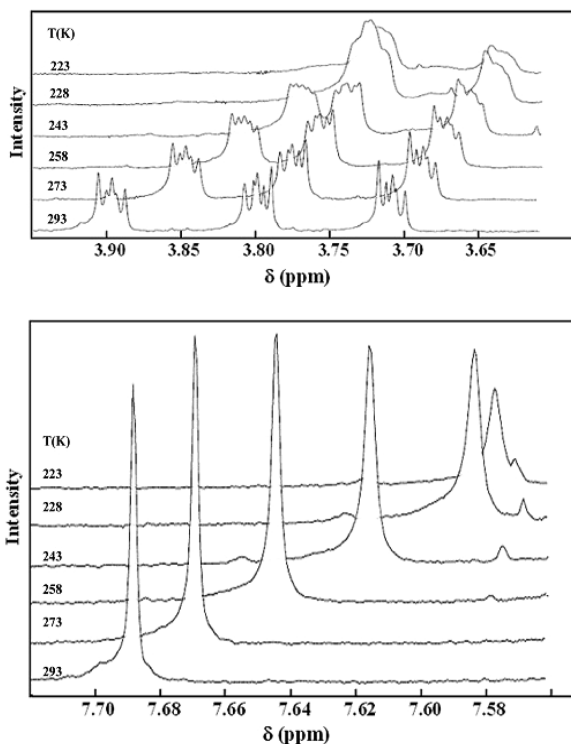
where \bar{E} represents an average over all reacting systems, and \bar{E} is an average over all systems, whether or not they react. Tolman's eq 9 states that the negative of the local slope of an Arrhenius plot will be equal to the average energy of molecules that react minus the average energy of all possible reactants. A convex Arrhenius plot means that \bar{E} decreases or that it increases less rapidly than as temperature increases. This model suggests new microscopic interpretations. It is assumed that the exchange in complex adopts two different states 1 and 2 at equilibrium, where state 2 is less reactive than state 1. In the less-reactive state 2, which dominates at lower temperatures, the rate constant of metal exchange is given by k_{2t} , whereas in the more reactive state dominating at higher temperatures, it is given by k_{1t} . At lower temperatures, the observed rate constant is smaller than the expected one. In addition, the observed pre-exponential factor is unusually large.

It is only at higher temperatures that the measurement of Arrhenius curve is true, which results in a normal pre-exponential factor. Limbach et al. explained this phenomenon in terms of the hydrogen-bond association of the reactants.^{41,42} There are also several reports available on the effect of hydrogen-bonding on stabilization of calixarenes in a especial conformation and also reduction of exchange rates because of

TABLE 2: Life Times, Calculated Rate Constants, and Activation Parameters for Intramolecular Exchange Mechanism in $R \geq 1$ from the Half Width of the $-OH$ Protons of L ($[L] = 0.002$ M)

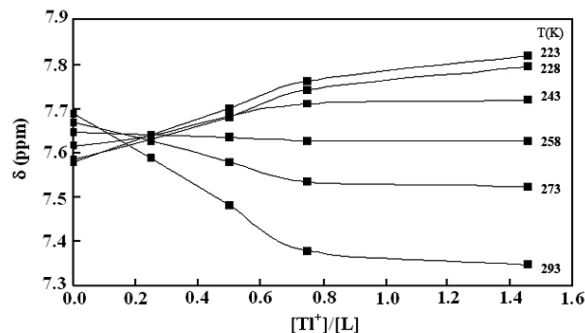
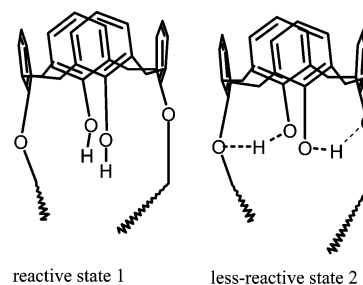
T (K)	τ (ms)				k_t (s^{-1})	activation parameters				
	$R = 1.0$	$R = 1.3$	$R = 1.5$	$R = 1.7$		A (Hz)	E_a (kJ/mol)	ΔH^\ddagger (kJ/mol)	ΔS^\ddagger (J/molK)	ΔG^\ddagger_{300} (kJ/mol)
223	265	150	214	216	2.8	1.49×10^{33a}	41.3 ^a	139.4 ^a	325.8 ^a	237.1 ^a
228	81.4	90.3	94.7	97.0	5.5					
243	24.2	21.7	22.2	22.8	22.0					
258	9.6	9.7	9.7	9.6	51.9	7.21×10^2 ^b	4.8 ^b	2.4 ^b	-197.0 ^b	61.5 ^b
273	5.6	5.2	5.1	5.4	93.6					
293	4.8	4.8	4.7	4.5	106.1					

^a Low temperature regime. ^b High temperature regime.

**Figure 10.** Arrhenius plot of Tl^+-L complex for $R \geq 1$.**Figure 11.** Temperature dependency of hydroxyl and OCH_2 signals of free L at different temperatures.

rigidifying of the host molecule.²⁸⁻³² Figure 11 shows the temperature dependency of hydroxyl and OCH_2 signals of ligand L . As can be seen, one of the OCH_2 signals is shifted as of OH signal shifts. This may be attributed to hydrogen-bonding effect.

Figure 12 shows the trend of chemical shift of the hydroxyl groups of the free ($R = 0$) and complexed L versus the metal/ligand mole ratio at different temperatures. Obviously, at the highest temperature of 293 K (curve 6), the signal shows an upfield shift with molar ratio, while at the lowest temperature of 223 K (curve 1) a downfield shift is observed with increasing R . In other words, the direction of chemical shift with metal/ligand mole ratio will

**Figure 12.** Trend of chemical shift of hydroxyl groups in calix[4]crown-6 vs mole ratio at different temperatures.**SCHEME 3: Proposed Conformer States of 1 and 2**

change from upfield at 293 K (curve 6) to downfield at 223 K (curve 1), so that at a middle temperature of 258 K (curve 4), the resulting mole ratio plot shows the lowest change in chemical shift (i.e., about 0.02 ppm) in the series, from $R = 0$ to $R = 1.35$. The observation at 258 K can be explained in two possible ways: (a) negligible interaction between thallium ion and L , and (b) temperature dependence of internal conversion of conformers. The hypothesis (a) is too hard to be accepted because of obvious significant interaction of the components. The hypothesis (b) assumes two conformer states of 1 and 2 as mentioned already. State 1 denotes the dominant conformer at high temperatures and state 2 to the less-reactive one at low temperatures (Scheme 3).

At low temperatures, the complex is in a rigid hydrogen-bonded state, and at high temperatures, dissociation of the hydrogen bonds of the complex occurs, and the temperature dependence of the observed rate constants may also be affected by the Gibbs free energy of the hydrogen-bond association. These two conformers experience different anisotropic and/or electron density by addition of thallium ion, and then two negative and positive trends are observed for this complexation. Hence, we thought the concentration independency of chemical shift at 258 K is because of the balance of electron density of states 1 and 2. The activation parameters for the two temperature regimes were evaluated by drawing tangents at the upper and lower temperature regimes of the Arrhenius plot (Figure 10), and the results are summarized in Table 2. The observation of smaller activation parameters for the high temper-

ature regime is in agreement with the destruction of hydrogen bonds and consequent compensation of the tunneling energy barrier. In addition, the unusually high activation parameters for the low temperature regime can be contributed to the formation of a rigid hydrogen bonded state.

Conclusion

The variable temperature proton NMR studies, in the range of 223–293 K, on the calix[4]crown-6–Tl⁺ system in a binary deuterated acetonitrile/chloroform (4:1v/v) mixture showed two coalescence temperatures at 243 and 228 K, corresponding to unimolecular and/or bimolecular and conformational transitions, respectively. The dynamic proton NMR spectroscopy at lower temperatures showed that the metal ion alternates intramolecularly between the two sides of the crown loop. A convex Arrhenius curve was observed, which indicate the tunneling of thallium ion through the hole of crown loop in the ligand because of two possible conformers of the complex.

Appendices

Appendix A: Evaluation of formation constant by ¹H NMR Spectroscopy.

The complexation of Tl⁺ cation by **L** in solvent is given by the eq 1.



$$K_f = [\text{Tl-L}^+]/[\text{Tl}^+][\text{L}] \quad (2)$$

where K_f is the formation constant of Tl⁺–**L** system. The use of Debye-Huckel limiting law of 1:1 electrolytes leads to the conclusion that $f(\text{Tl}^+)$ and $f(\text{Tl-L}^+)$, so that the activity coefficients in eq 2 cancel out. The proton chemical shifts were monitored as a function of [Tl⁺]/[**L**] mole ratio in solution (eq 1). The formation constants of 1:1 Tl⁺–**L** complex were calculated from the variation of the proton chemical shift with [Tl⁺]/[**L**] mole ratio. It has been shown that in solution containing fixed concentration of **L**, and varying amount of Tl⁺ ion, the observed chemical shift of the proton is given by following equations:

$$\delta_{\text{obs}} = P_{\text{L}}\delta_{\text{L}} + P_{\text{complex}}\delta_{\text{complex}} \quad (3)$$

where P_{L} and P_{complex} are the mole fractions of the free and complexed ligand, respectively. By substitution from eq 2 and the mass balance equation $C_{\text{L}} = [\text{L}] + [\text{Tl-L}^+]$, eq 3 can be written as:

$$\delta_{\text{obs}} = \{[K_f C_{\text{Tl}} - K_f C_{\text{L}} - 1] + (K_f^2 C_{\text{Tl}}^2 + K_f^2 C_{\text{L}}^2 - 2K_f^2 C_{\text{L}} C_{\text{Tl}} + 2K_f C_{\text{Tl}} + 2K_f C_{\text{L}} + 1)^{1/2}\} \times (\delta_{\text{L}} - \delta_{\text{complex}})/2K_f C_{\text{Tl}} + \delta_{\text{complex}} \quad (4)$$

where C_{L} and C_{Tl} are total concentrations of the **L** and Tl⁺ ion, respectively, and δ_{L} and δ_{complex} are the respective chemical shifts of the free and complexed ligand. The nonlinear least-squares curve fitting program was used to evaluate K_f and δ_{complex} values by fitting the δ_{obs} versus C_{Tl} data.²⁵

Appendix B: Evaluation of Formation Constant by Conductometry.

The molar conductances, Λ_{obs} , in (S cm² mol⁻¹) can be calculated by using the following equation:

$$\Lambda_{\text{obs}} = 1000k/C_{\text{Tl}} \quad (5)$$

where k is the conductance of the test solution in S cm⁻¹. The formation constants, K_f , in terms of the molar conductance can be expressed as:

$$K_f = [\text{Tl-L}^+]/[\text{Tl}^+][\text{L}] = (\Lambda_{\text{Tl}} - \Lambda_{\text{obs}})/(\Lambda_{\text{obs}} - \Lambda_{\text{complex}})[\text{L}] \quad (6)$$

$$[\text{L}] = C_{\text{L}} - \{C_{\text{Tl}} - (\Lambda_{\text{Tl}} - \Lambda_{\text{obs}})/(\Lambda_{\text{obs}} - \Lambda_{\text{complex}})\} \quad (7)$$

Here, Λ_{Tl} is the molar conductance of the metal ion before addition of ligand, Λ_{complex} is the molar conductance of the complexed ion, and Λ_{obs} is the molar conductance of the solution during titration. The formation constants, K_f , and the molar conductance of the complex, Λ_{complex} , were evaluated by computer fitting of eqs 6 and 7 to the molar conductance [L]/[Tl⁺] mole ratio data using a nonlinear least-squares program.

Appendix C: Two-Site Exchange Equations.

The general case of exchange between the two sites A (free ligand) and B (complexed ligand) with different relaxation times is described by the following modified Bloch equation.²²

$$G = u + iv \quad (2)$$

$$v = -\gamma H_1 M_0 (SU + TV)/(S^2 + T^2) \quad (3)$$

$$u = -\gamma H_1 M_0 (UT + SV)/(S^2 + T^2) \quad (4)$$

where G is the complex moment of magnetization, and v and u are the pure absorption and pure dispersion line shapes, respectively. The γ , H_1 , and M_0 are the gyromagnetic ratio, field strength, and macroscopic magnetization, and

$$S = P_A/T_{2A} + P_B/T_{2B} + \tau/T_{2A}T_{2B} - \tau(\omega_A - \omega)(\omega_B - \omega) \quad (5)$$

$$U = 1 - \tau(P_B/T_{2A} + P_A/T_{2B}) \quad (6)$$

$$T = (P_A\omega_A + P_B\omega_B - \omega) + \tau[(\omega_A - \omega)/T_{2B} + (\omega_B - \omega)/T_{2A}] \quad (7)$$

$$V = \tau(P_B\omega_A + P_A\omega_B - \omega) \quad (8)$$

where P_A and P_B are the relative population at sites A and B, respectively; ω_A and ω_B are the resonance frequencies at the two sites in the absence of exchange; and T_{2A} and T_{2B} are the respective relaxation times at each site in the absence of exchange. The τ is the mean lifetime of the exchange processes defined by

$$\tau = \tau_A \tau_B / (\tau_A + \tau_B) \quad (9)$$

where τ_A and τ_B represent the mean residence times of the on sites A (free ligand) and B (complexed), respectively.

The shape function, adapted for our case of Fourier-transform spectroscopy, may be written as follows:

$$I(\nu) = I_0(u \sin \theta + v \cos \theta) + b \quad (10)$$

where I_0 , θ , and b are the amplitude, phase correction, and baseline, respectively.

Acknowledgment. This work has been supported by grants from the Tarbiat Modares University Research Council, which is hereby gratefully acknowledged.

References and Notes

- (1) Gutsche, C. D. *Calixarenes*; Royal Society of Chemistry: Cambridge, U.K., 1989.
- (2) Vicens, J.; Böhmer, V. *Calixarenes: A Versatile Class of Macrocyclic Compounds*; Kluwer Academic Publishers: Dordrecht, Boston, 1991.
- (3) Ikeda, A.; Shinkai, S. *Chem. Rev.* **1997**, *97*, 1713–1734.
- (4) Casnati, A.; Pochini, A.; Ungaro, R.; Ugozzoli, F.; Arnaud, F.; Fanni, S.; Schwing, M.-J.; Egberink, R. J. M.; de Jong, F.; Reinhoudt, D. N. *J. Am. Chem. Soc.* **1995**, *117*, 2767–2777.
- (5) Dijkstra, P. J.; Brunink, J. A. J.; Bugge, K.-E.; Reinhoudt, D. N.; Harkema, S.; Ungaro, R.; Ugozzoli, F.; Ghidini, E. *J. Am. Chem. Soc.* **1989**, *111*, 7567–7575.
- (6) Ghidini, E.; Ugozzoli, F.; Ungaro, R.; Harkema, S.; El-Fadl, A. A.; Reinhoudt, D. N. *J. Am. Chem. Soc.* **1990**, *112*, 6979–6985.
- (7) Bohmer, V. *Angew. Chem., Int. Ed. Engl.* **1995**, *34*, 713–745.
- (8) Mueller, P.; Rudin, D. O. *Biochem. Biophys. Res. Commun.* **1967**, *26*, 398–404.
- (9) Henderson, P. J.; McGivan, J. D.; Chappell, J. B. *Biochem. J.* **1969**, *111*, 521–535.
- (10) Sandeaux, R.; Sandeaux, J.; Gavach, C.; Brun, B. *Biochim. Biophys. Acta (BBA)—Biomembranes* **1982**, *684*, 127–132.
- (11) Cox, B. G.; Schneider, H. *Coordination and Transport Properties of Macrocyclic Compounds in Solution*; Elsevier: Amsterdam, New York, 1992.
- (12) Atwood, J. L.; Lehn, J. M. *Comprehensive Supramolecular Chemistry*; Pergamon: New York, 1996.
- (13) Roper, E. D.; Talanov, V. S.; Gorbunova, M.; Bartsch, G. R. A.; Talanova, G. G. *Anal. Chem.* **2007**, *79*, 1983–1989.
- (14) Roper, E. D.; Talanov, V. S.; Butcher, R. J.; Talanova, G. G. *Supramol. Chem.* **2008**, *20*, 217–229.
- (15) Mohammed-Ziegler, I. *Spectrochim. Acta Part A* **2003**, *59*, 19–27.
- (16) Talanova, G. G.; Roper, E. D.; Buie, N. M.; Gorbunova, M. G.; Bartsch, R. A.; Talanov, V. S. *Chem. Commun.* **2005**, 5673–5675.
- (17) Matthews, S. E.; Rees, N. H.; Felix, V.; Drew, M. G. B.; Beer, P. D. *Inorg. Chem.* **2003**, *42*, 729–734.
- (18) Felix, V.; Matthews, S. E.; Beer, P. D.; Drew, M. G. B. *Phys. Chem. Chem. Phys.* **2002**, *4*, 3849–3858.
- (19) Meier, U. C.; Detellier, C. *J. Phys. Chem. A* **1998**, *102*, 1888–1893.
- (20) Coetzee, J. F.; Campion, J. J. *J. Am. Chem. Soc.* **1967**, *89*, 2513–2517.
- (21) Asfari, Z.; Nicolle, X.; Vicens, J.; Dozol, J. f.; Duhart, A.; Harrowfield, J. M.; Skelton, B. W.; White, A. H. *J. Incl. Phenom. Macrocycl. Chem.* **1999**, *33*, 251–262.
- (22) Pople, J. A.; Schneider, W. G.; Bernstein, H. J. *High-Resolution Nuclear Magnetic Resonance*; McGraw-Hill: New York, 1959.
- (23) Mulkey, J. P.; Oehme, F. W. *Vet. Human Toxicol.* **1993**, *35*, 445–454.
- (24) Glaser, J. *Adv. Inorg. Chem.* **1995**, *43*, 1–69.
- (25) Roach, E. T.; Handy, P. R.; Popov, A. I. *Inorg. Nucl. Chem. Lett.* **1973**, *9*, 359–363.
- (26) Jankowski, C. K.; Hocquet, C.; Arseneau, S.; Moulin, C.; Mauclair, L. *J. Photochem. Photobiol. A: Chem.* **2006**, *184*, 216–220.
- (27) Jankowski, C. K.; Van Calsteren, M. R.; Aychet, N.; Dozol, J. F.; Moulin, C.; Lamouroux, C. *Can. J. Chem.* **2005**, *83*, 1098–1113.
- (28) Koehler, J. E. H.; Saenger, W.; Gunsteren, W. F. *Eur. Biophys. J.* **1988**, *16*, 153–168.
- (29) Janssen, R. G.; vanDuynhoven, J. P. M.; Verboom, W.; vanHummel, G. J.; Harkema, S.; Reinhoudt, D. N. *J. Am. Chem. Soc.* **1996**, *118*, 3666–3675.
- (30) Conner, M.; Janout, V.; Regen, S. L. *J. Am. Chem. Soc.* **1991**, *113*, 9670.
- (31) Guelzim, A.; Saadioui, M.; Asfari, Z.; Vicens, J. *J. Incl. Phenom. Macrocycl. Chem.* **2001**, *39*, 91–95.
- (32) Gutsche, C. D. *Acc. Chem. Res.* **1983**, *16*, 161–170.
- (33) Alizadeh, N.; Bordbar, M.; Shamsipur, M. *Bull. Chem. Soc. Jpn.* **2005**, *78*, 1763–1772.
- (34) Meier, U. C.; Detellier, C. *J. Phys. Chem. A* **1999**, *103*, 3825–3829.
- (35) Amini, M. K.; Shamsipur, M. *J. Phys. Chem.* **1991**, *95*, 9601.
- (36) Ikeda, A.; Tsudera, T.; Shinkai, S. *J. Org. Chem.* **1997**, *62*, 3568.
- (37) Truhlar, D. G.; Kohen, A. *Proc. Natl. Acad. Sci. U.S.A.* **2001**, *98*, 848–851.
- (38) Wrba, A.; Schweiger, A.; Schultes, V.; Jaenicke, R.; Zavodszky, P. *Biochem.* **1990**, *29*, 7584–7592.
- (39) Koehn, E. M.; Fleischmann, T.; Conrad, J. A.; Palfey, B. A.; Lesley, S. A.; Mathews, I. I.; Kohen, A. *Nature* **2009**, *458*, 919–923.
- (40) Kohen, A.; Cannio, R.; Bartolucci, S.; Klinman, J. P. *Nature* **1999**, *399*, 496–499.
- (41) Limbach, H. H.; Lopez, J. M.; Kohen, A. *Phil. Trans. R. Soc. B* **2006**, *361*, 1399–1415.
- (42) Limbach, H. H.; Mannel, F.; Detering, C.; Denisov, G. S. *Chem. Phys.* **2005**, *319*, 69–92.
- (43) Tolman, R. C. *J. Am. Chem. Soc.* **1920**, *42*, 2506–2528.
- (44) Tolman, R. C. *Statistical Mechanics with Applications to Physics and Chemistry*; The Chemical Catalog Company, Inc.: New York, 1927.
- (45) Truhlar, D. G. *J. Chem. Educ.* **1978**, *55*, 309–311.